



Statistical Modeling of Urban Heat Island Intensity in Warsaw, Poland Using Simultaneous Air and Surface Temperature Observations

Lech Gawuc , Maciej Jefimow, Karol Szymankiewicz , Magdalena Kuchcik, Anahita Sattari, and Joanna Struzewska

Abstract—Urban heat island (UHI) is one of the most distinctive characteristics of urban climate. The objective of this study is to apply a statistical modeling of the nocturnal atmospheric UHI based on the relationship between observed air temperature from ground stations and remotely sensed temperature of the urban surface. The goal of the approach is to limit input data for the developed modeling method in order to assure transferability of the methodology in different cities. Time series of surface temperature and normalized difference vegetation index are obtained from the MODIS instrument for a 10-year period (2008–2017). The air temperature is collected from the *in-situ* observational network of 21 stations. The studies are conducted for different locations with gradual changes in urbanization in order to assess the impact of urbanization on the relationship between simultaneous air and surface UHI. The urbanization is described by commonly available land cover metrics. Results showed that the proposed approach provides satisfactory AUHI modeling results for the locations with the least degree of urbanization. The best results are obtained with a simple linear regression model with the iterative procedure to minimize the mean absolute gross error (MAGE). The lowest MAGE for modeled UHI is 1.18 °C with 69% of the variance explained. The strongest linear relationship between simultaneous SUHI and AUHI is noted for those station pairs whose surroundings have the highest differences in urbanization, and the highest UHI intensities are observed. The strength of the SUHI/AUHI linear relationship decreases gradually with the increasing urbanization of the stations' surroundings.

Index Terms—Air temperature (AT), prediction, regression, statistical modeling, surface temperature, urban climate, urban heat island (UHI).

Manuscript received October 30, 2019; revised February 23, 2020; accepted April 10, 2020. Date of publication June 1, 2020; date of current version June 11, 2020. The work of L. Gawuc was supported by the National Science Centre (Poland) under Grant “Preludium” (2016/21/N/ST10/00430). (Corresponding author: Lech Gawuc.)

Lech Gawuc and Karol Szymankiewicz are with the Institute of Environmental Protection—National Research Institute, 00-548 Warsaw, Poland (e-mail: lech.gawuc@kobize.pl; karol.szymankiewicz@kobize.pl).

Maciej Jefimow and Joanna Struzewska are with the Faculty of Building Services Hydro, and Environmental Engineering, Warsaw University of Technology, 00-653 Warsaw, Poland (e-mail: maciej.jefimow@pw.edu.pl; joanna.struzewska@pw.edu.pl).

Magdalena Kuchcik is with the Institute of Geography and Spatial Organization, Polish Academy of Sciences, 00-818 Warsaw, Poland (e-mail: mkuchcik@twarda.pan.pl).

Anahita Sattari is with the Institute of Geophysics, Polish Academy of Sciences, 01-452 Warsaw, Poland (e-mail: asattari@igf.edu.pl).

Digital Object Identifier 10.1109/JSTARS.2020.2989071

NOMENCLATURE

Abbreviations

AT	Air temperature.
AUHI	Air urban heat island.
CC	Pearson correlation coefficient.
DSM	Digital surface model.
EEA	European Environmental Agency.
ISA	Impervious surface area.
LCZ	Local climate zone.
LST	Land surface temperature.
LU/LC	Land use/land cover data.
MAGE	Mean absolute gross error.
MAGE/avAUHI ratio	Ratio between the MAGE and the average AUHI intensity calculated for the station group.
mAUHI	Modeled air (canopy) urban heat island.
MBE	Mean bias error.
ML	Multiple linear regression model.
MODIS	Moderate resolution imaging spectroradiometer.
MSL	Simple linear regression model with iteratively minimized MAGE.
NDVI	Normalized difference vegetation index.
oAUHI	Observed air (canopy) urban heat island.
oSUHI	Observed surface urban heat island.
R^2	Coefficient of determination.
RMSE	Root-mean-square error.
PAS	Polish Academy of Sciences.
SD ratio	Ratio between the standard deviation of mAUHI and oAUHI.
SEB	Surface energy balance.
SL	Simple linear regression model.
SUHI	Surface urban heat island (general term).
SVF	Sky view factor.
UA “rural”	Combined EEA Urban Atlas classes: (14100) Green urban areas, (14200) Sports and leisure facilities, (23000) Pastures, (31000) Forests.

UA “urban”	Combined EEA Urban Atlas classes: (11100) Continuous Urban fabric, (11210) Discontinuous Dense Urban Fabric.
UHI	Urban heat island (general term).
z0	Roughness height for momentum.

I. INTRODUCTION

URBAN areas are highly heterogeneous regarding parameters, such as surface roughness, sky view factor (SVF), aspect ratio (wall-to-building height), imperviousness, vegetation cover and vegetation type, albedo, and depth and function of underground infrastructure. Since the character of urban wind flow is significantly altered, compared to rural areas, the turbulent surface–air energy exchange in cities is very complicated. Therefore, given the character of urban areas, observing and modeling the urban surface energy balance (SEB—all abbreviations are listed in Nomenclature) is challenging. An altered SEB is the genesis of the UHI phenomenon [1].

Urban heat island (UHI) is one of the most distinct singularities of urban climate. UHI is defined as the difference in temperature between urban and rural areas. It can be divided into several categories, depending on the kind of temperature analyzed: air, surface, or soil [2]. The most common approach is to utilize *in-situ* air temperature (AT) measurements conducted at stationary stations. Different heights are utilized for measurement purposes, i.e., ground level [3], [4] or roofs [5], while some studies also utilize mobile platforms [6], [7]. Using *in-situ* AT data for the UHI analysis involves a significant disadvantage since it does not directly provide a spatial pattern of urban temperature, which is highly heterogeneous. Therefore, appropriate localization of observational sites is critical [8], [9].

To overcome the limitation of spatial representativeness in the case of *in-situ* air observations, many studies utilize remotely sensed land surface temperature (LST) in urban climate research. Satellite sensors allow for an instantaneous observation of LST over vast areas. If the surface temperature is used, “surface” UHI can be discussed [10]. Thermal satellite data are typically obtained from sun-synchronous orbits, which means that only a few acquisitions of the same target are possible per day (for MODIS, two per day per one platform). This is further hampered by cloudiness conditions. Consequently, all of the reported investigations are inevitably limited to the very moment of satellite overpass [11]. Moreover, thermal remote sensing data are prone to angular thermal anisotropy [12] or the impact of earth–satellite geometry on the atmospheric paths [13]. Therefore, appropriately interpreting urban thermal measurements remains challenging.

All of the meteorological characteristics are highly variable in space and time, especially in urban areas. Hence, using only satellite data or analyzing only selected seasons is not enough to fully understand the singularities of urban micrometeorological environment. The solution to partially overcome the limitations caused by the nature of instantaneous satellite observations is to employ temporal compositions [14], [15] or fusion techniques [16].

Despite significant shortcomings, thermal satellite remote sensing has been widely used to investigate the links between LST and characteristics of urban land use/land cover (LU/LC) [17], [18] or SEB [19]–[21]. The relation between LST and indirectly described human activity or population characteristics has also been studied [22]–[24].

Although AT is the parameter that has the most apparent impact on human health [25], [26], LST is particularly useful when developing urban heat mitigation strategies [27]. Therefore, using simultaneous *in-situ* and remote sensing data allows for comprehensive analyses of UHI.

A. Studies on Simultaneous AUHI and SUHI

One of the first studies to employ extensive *in-situ* AT measurements along with satellite remote sensing data was the work of Nichol and Wong [28]. In that paper, the authors used one ASTER image and traverse observations from mobile platforms with a length of about 130 km in the city of Hong Kong, China. The study examined the spatial variability of AT corresponding to different degrees of urbanization on a winter’s night. In another paper focused on Hong Kong, it was also demonstrated that thermal satellite images combined with *in-situ* ground data could be used to more fully understand the genesis of the altered urban thermal environment [29]. Sheng *et al.* [30] compared air UHI (AUHI) and surface UHI (SUHI) using fifteen Landsat 5 images and five *in-situ* stations for the city of Hangzhou, China. It was concluded that AUHI and SUHI intensities are very different and cannot be compared. In Europe, Schwarz *et al.* [31] systematically quantified SUHI and AUHI indicators for the city of Leipzig, Germany. Analysis of the relationship between the land surface and ATs was presented. The authors recommended using several SUHI/AUHI indicators in parallel in order to acknowledge the uncertainty while using a single indicator. Majkowska *et al.* [32] reported that SUHI and AUHI are common phenomena in Poznań, Poland. It was found that the AUHI mean annual intensity was 1.0 °C. Moreover, results based on remote sensing data and the Corine Land Cover 2006 database indicate that the highest value of mean LST anomalies (3.4 °C) was attained by the continuous urban fabric, whereas the lowest value occurred within broad-leaved forests (−3.1 °C). This is consistent with the results of the analysis of spatial patterns of simultaneous AUHI and SUHI in Birmingham, U.K., which suggest that the canopy UHI is more related with the advection processes, whereas SUHI is more dependent on the land use [33]. For the same city, Zhang *et al.* [34] obtained similar intensities of AUHI and SUHI but the correlation coefficient (CC) describing their relationship was found weak (0.41). Only a limited amount of satellite images was utilized (77 MODIS images) covering selected weather types. Moreover, due to the utilization of only two *in-situ* stations, it was impossible to conclude on the impact of urban morphology on the SUHI–AUHI relationship fully.

Easy access to satellite LST observations is especially relevant to the study of urban climate in cities with no or sparse *in-situ* observational networks. However, remote sensing techniques are incapable of providing AT and AUHI intensity values directly.

For such purpose, statistical modeling methods might be helpful, since they can provide an approximated AT or AUHI intensities. This might be very useful for urban parameterizations used for mesoscale modeling.

B. AUHI Modeling Based on Empirical Parameters

One of the first statistical methods to predict AUHI intensity was proposed by Oke [35]. The AUHI intensity was found to be approximately proportional to the fourth root of the population for North American cities. In a later paper [36], the AUHI model was generalized and related to SVF. In Europe, Bottyán and Unger [6] estimated the spatial distribution of the mean AUHI intensity using urban surface parameters in Szeged, Hungary. A strong linear relationship between the mean maximum AUHI intensity and parameters, such as SVF, building height, built-up ratio, or water surface ratio, was found. Brandsma and Wolters [37] conducted transect measurements in the city of Utrecht, Netherlands, to model the spatial distribution of mean and maximum nighttime AUHI intensity and to relate them to area-averaged SVFs and land use combined at both the micro- and local scales. Hoffman *et al.* [38] presented a linear regression model for nocturnal AUHI prediction based on meteorological parameters, such as cloud cover, wind speed, and relative humidity. Theeuwes *et al.* [39] proposed a diagnostic equation for the daily maximum AUHI prediction using dimensional analysis. The equation was further improved for Asian cities [40]. Recently, Straub *et al.* [41] applied multiple linear regression and random forest methods to derive AT spatial patterns in a heterogeneous urban area. LU/LC characteristics were applied as predictors and a dense observational network, which consisted of 77 locations across the city of Augsburg, Germany.

C. Aim of the Presented Study

The objective of the presented study was to apply the AUHI/SUHI relationship for the statistical modeling of AUHI. Many previous works apply different statistical modeling techniques for UHI prediction, but most of them require data that are difficult to obtain.

The initial step of our approach was to find appropriate *in-situ* AT measurements posts, which represent the most typical urban features. Ground station described by LU/LC metrics driven from remote sensing observations (LST, surface imperviousness—ISA and normalized difference vegetation index—NDVI) were used here in the AUHI modeling. Since typically the biggest issue with appropriate AUHI evaluation is the lack of sufficiently dense measuring networks of AT (such as this from Warsaw) and the second goal was to limit input data in order to assure transferability of the methodology for different cities. Here, commonly available remote sensing observations were used along with simultaneous *in-situ* measurements, which were restricted to AT only. A simple method for AUHI intensity prediction was presented. We aimed to verify the feasibility of such an approach for a practical application by analyzing if satisfactory results of modeled UHI can be obtained.

The choice of rural sites is a key step for any UHI studies [42], [43], hence it is also critical for any AUHI/SUHI relationship

analysis. The problem was addressed in the presented study, by calculating surface and air UHI intensities for 20 locations across the city covering different LU/LC.

In total, 442 MODIS (MOD/MYD11L2) images were used for the period 2008–2017. A significant amount of the input data collected over 10 years guarantees that the impact of incidental synoptic conditions was avoided and the seasonal meteorological differences are blended. Such an approach provides clarity and facilitates interpretation of the obtained results, especially taking into account the limitations of thermal satellite data or seasonal variability of UHI intensity.

II. DATA AND METHODS

A. Target Area—The City of Warsaw

Warsaw is the capital and the largest city of Poland. The whole city agglomeration is home to more than 2 500 000 citizens. It is located in the center of the country and the River Vistula, the largest river in Poland, runs through it.

Its area of almost 515 km² has significant differentiation of LU/LC. Currently, about 248 km² is the built-up area (48%). Within this, considerable part (about 57 km²) is covered by industry, trade units, and transport systems. Forests make up about 15% of the city. Urban parks and other recreational green areas cover 10%. 12% of the city territory is used as arable land, for crops and pasture. The category “heterogeneous agricultural areas” includes sparsely built areas and allotment gardens—11.3% (Corine Land Cover 2007).

The recent tendency in the city development is to build densely settled residential districts, and, also, to insert new buildings into free spaces in the city center (which was dramatically destroyed during the World War II). For the whole city, there is only a general overview of investment intentions (Council of Warsaw, Legal act LXII/1667/2018, 2018).

The city of Warsaw is located on flat terrain—the difference between the highest and lowest point is only 43 m. Western and southwestern winds are prevailing in the city. The main ventilation corridor is the river Vistula valley that crosses the agglomeration in a diagonal axis (southeastern to northwestern).

B. AT Observational Network

The Polish Academy of Sciences microclimatic measurements network started operations in Warsaw agglomeration in 1998 with three posts. Then, it was developed to 13 locations in 2006, and to 40 over the years 2011–2014. Later, it was limited to 27 in 2016 and 20 stations in 2018. Onset HOBO temperature data loggers are situated in white, openwork covers 2 m above the grassy ground. The locations represent different LU/LC, different ratios of biologically vital areas, surface imperviousness, SVF, etc. Data are collected with a 10-min logging interval. Stations are located in various places covering different grades of urbanization. Currently, this is the densest urban AT observational network in Poland. The abundance of the measurements allows us to choose stations located in such urban microenvironments, which are typical for Polish cities. Hence, the presented methodology has a potential to be transferred and

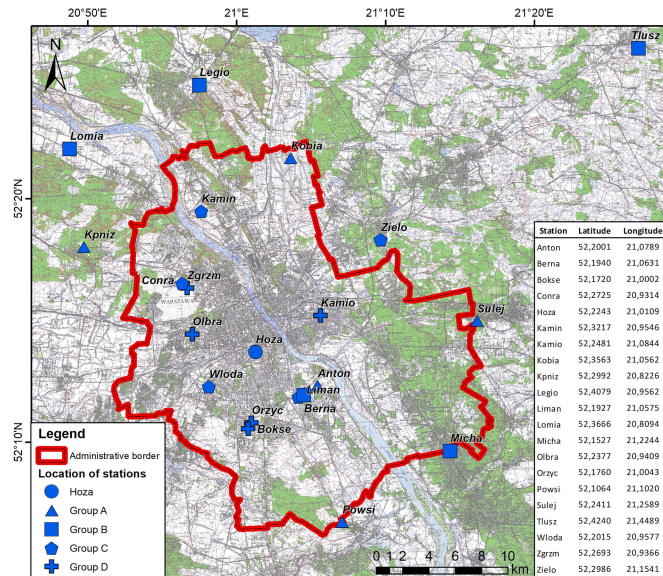


Fig. 1. Locations of the ground stations.

applied in other cities. Fig. 1 shows the locations of the *in-situ* stations.

The PAS network was used in a number of projects and studies regarding temporal and spatial variability of UHI under the spatial development changes [45], methods for UHI mitigation and adaptation [46], [47], the impact of biologically vital areas on climate of housing estates [48], local climate zones (LCZs) [49], forecasts for the UHI based on selected climate change models, and scenarios of spatial development changes [50].

C. Selection of Simultaneous In-Situ and Satellite Data

The key to data choice for the experiment was a simultaneousness of direct ground and indirect satellite observations. From all freely available satellite data from various sensors, we chose the MODIS instrument onboard Terra and Aqua satellite. MODIS is the best compromise between temporal and spatial resolution for this research. We utilized nighttime MODIS MOD/MYD11_L2 products. Only images acquired from 35° off-nadir or less during periods of low cloudiness were selected. For the 10 years during 2008–2017, 442 nighttime images were obtained.

In this article, we considered only nighttime cases. The AT–surface temperature and therefore AUHI–SUHI relationship is much more complex during daytime as compared to nighttime, which is partially linked with the lower impact that thermal anisotropy has on nighttime thermal imagery [12]. Since daytime Terra and Aqua overpasses take place in the morning, some locations of *in-situ* stations might be shadowed and surrounding urban structures might be much cooler than during the nighttime overpass. This is especially important for the stations with high SVF. Therefore, the nighttime analyses are more representative, especially for long-term analyses.

Satellite observations were collected between 20:50 and 00:30 UTC. As the ground measurements were recorded every 10 min, the maximum time difference between satellite and *in-situ* observations was 5 min. MODIS LST pixels from each satellite

TABLE I
NUMBER OF UTILIZED SATELLITE IMAGES, PIXELS, AND GROUND DATA SAMPLES

year	number of images	number of satellite pixels obtained	number of <i>in-situ</i> data samples
2008	42	895	617
2009	40	852	699
2010	48	1018	944
2011	50	1059	1092
2012	57	1217	1213
2013	43	916	904
2014	42	897	794
2015	42	892	821
2016	36	763	721
2017	42	901	801

image were matched with the locations of PAS *in-situ* stations using the nearest neighbor approach.

The number of samples available for each year was different. Table I shows the number of satellite images, the number of LST pixels obtained for *in-situ* station locations, and ground data samples collected for each year. The temporal distribution of data samples is uneven. Over the 10-year period, some stations were temporarily switched off due to calibration, maintenance, and modernization. Second, specific seasons in certain years may have had very different conditions regarding cloudiness. This is typical for the transitional climate of Poland.

In Section III-C, we present analyses of statistical modeling of AUHI using a multiple linear regression model (ML). The model coefficients were built using observed AUHI (oAUHI) and observed SUHI (oSUHI) values and NDVI time series, which were retrieved from MOD/MYD13A1 product. We utilized all products available for the period of the analyses and matched them with appropriate pairs of AT and LST observations.

D. Methodology for Matching Stations Into Pairs and Groups

According to the definition of the UHI phenomenon and the common difficulties with differentiation between urban and rural areas, it was critical to match appropriate locations in “urban point–rural point” pairs. In Table II, we present LU/LC descriptions for all locations. In order to highlight the impact of urbanization on the relationship between oSUHI and oAUHI, the location with the most urbanized surroundings (Hoza) was selected as the “urban reference.” All other remaining locations were considered as “rural reference”, not referring to their physical characteristics but meaning that the air and surface temperature values observed at those stations were subtracted from that measured at Hoza. In order to maintain clarity, we used the term “the second item of UHI pair” instead of “rural reference.”

TABLE II
LU/LC STATISTICS FOR THE STATIONS' SURROUNDINGS

	No.	Station	ISA	NDVI	z0	LCZ	UA "urban"	UA "rural"	SVF	1-NDVI+ISA
Group D (urban stations)	1	Hoza	0.73	0.32	0.73	2	0.91	0.00	25	1.41
	2	Orzyc	0.44	0.42	0.36	5	0.70	0.06	13	1.02
	3	Kamio	0.47	0.46	0.28	5	0.88	0.00	50	1.01
	4	Olbra	0.44	0.47	0.34	4	0.85	0.00	48	0.97
	5	Bokse	0.40	0.47	0.25	5	0.65	0.00	26	0.93
	6	Zgrzm	0.41	0.50	0.19	6	0.73	0.00	63	0.91
Group C (sub-urban 1)	7	Liman	0.40	0.53	0.24	5	0.43	0.12	37	0.87
	8	Conra	0.34	0.53	0.28	4	0.59	0.13	24	0.81
	9	Wloda	0.31	0.52	0.20	5	0.56	0.29	35	0.79
	10	Kamin	0.36	0.59	0.26	5	0.53	0.22	74	0.77
	11	Zielo	0.38	0.63	0.28	6	0.87	0.00	70	0.75
Group B (sub-urban 2)	12	Micha	0.24	0.60	0.42	B	0.61	0.29	63	0.64
	13	Berna	0.22	0.59	0.27	4	0.57	0.28	57	0.63
	14	Legio	0.22	0.60	n/a	D	0.26	0.52	72	0.62
	15	Lomia	0.14	0.58	n/a	C	0.00	0.73	81	0.56
	16	Thusz	0.20	0.68	n/a	9	0.54	0.34	69	0.52
Group A (rural stations)	17	Anton	0.14	0.68	0.17	9	0.16	0.72	74	0.46
	18	Powski	0.13	0.68	0.26	B	0.48	0.42	73	0.45
	19	Kobia	0.05	0.67	0.19	9	0.36	0.51	62	0.38
	20	Sulej	0.04	0.66	0.35	9	0.18	0.77	77	0.38
	21	Kpniz	0.07	0.77	0.71	A	0.40	0.58	82	0.30

“Point to point” definition of UHI is the most straightforward approach (see Schwarz *et al.* [51]). In light of the aim of the presented study, it allows for a comprehensive and consistent analysis of the impact of urbanization for UHI intensities and in particular analysis of the α AUHI/ α SUHI relationship.

All the locations considered as the second item of UHI pair were combined into four groups with gradual changes in the surroundings as described by ISA, NDVI, z0 (roughness height for momentum), and Urban Atlas classes (combined into an urban and rural the category—see Nomenclature), LCZs and SVF (see Table II).

Each group consists of five locations. The locations group A represents the least urbanized surroundings, and group D consists of the locations with the most urbanized surroundings. In order to put locations into groups, we propose an original and yet simple parameter: 1-NDVI+ISA. ISA was obtained from the Copernicus Services, and NDVI was calculated as a 10-year (2008–2017) mean from time series of MODIS MOD/MYD13Q1 product. 1-NDVI+ISA parameter is simple, based on commonly used and available data and it conveniently combines information on vegetation and surface imperviousness. Group A consists of stations for which the 1-NDVI+ISA parameter has values below 0.50, group B—0.50–0.70, group C—0.70–0.90, and group D—0.90–1.10. The station considered

as “urban reference” (Hoza) has the 1-NDVI+ISA parameter of 1.41—much higher than all other stations.

All of the parameters presented in Table II were calculated within a buffer of 250 m around the stations in the longitudinal and latitudinal directions. The roughness height for momentum (z0) was calculated using a relationship equal to $0.1 \times$ mean height of roughness elements [52]. Z0 was calculated by means of digital surface model (DSM) which included vegetation. SVF values and LCZs were adopted from [49].

E. α AUHI/ α SUHI Relationship for Statistical Modeling of m AUHI

The first step in this part of the research was to test three versions of the linear regression model. First, we tested a simple linear regression model (SL) with a directional coefficient and intercept taken directly from the observations of α AUHI and α SUHI. Second, we applied an ML using α AUHI and α SUHI and time series of NDVI values for each station. Third, we applied a simple linear regression model with an iterative procedure (MSL). The iteration was changing a directional coefficient of the regression function in order to obtain the best fit of the m AUHI. The intercept was kept constant and adopted from the SL. For each case, mean bias error (MBE), root-mean-square

TABLE III
OBTAINED CC, oAUHI, AND oSUHI VALUES FOR ALL STATIONS PAIRS

	No.	Station	oAUHI/oSUHI CC for pair Hoza and:	mean CC for a group:	10 yr mean oAUHI [°C]	10 yr mean oSUHI [°C]	10 yr mean oAUHI for group [°C]	10 yr mean oSUHI for group [°C]
Group D (urban stations)	2	Orzyc	0.46		1.15	0.62		
	3	Kamio	0.37		1.28	0.79		
	4	Olbra	0.47		1.14	0.45		
	5	Bokse	0.44		1.70	0.85		
	6	Zgrzm	0.62	0.47	1.65	0.64	1.38	0.67
	Group C (sub-urban 1)	7	Liman	0.57		1.93	1.30	
8		Conra	0.59		1.68	0.73		
9		Wloda	0.54		2.02	0.75		
10		Kamin	0.49		2.19	0.62		
11		Zielo	0.78	0.59	3.44	1.90	2.25	1.06
Group B (sub-urban 2)	12	Micha	0.66		4.49	1.72		
	13	Berna	0.59		3.29	1.47		
	14	Legio	0.62		3.46	2.34		
	15	Lomia	0.72		3.63	3.70		
	16	Tlusz	0.73	0.66	3.98	4.21	3.77	2.69
Group A (rural stations)	17	Anton	0.71		4.16	2.42		
	18	Powosi	0.69		4.19	3.30		
	19	Kobia	0.83		4.73	4.29		
	20	Sulej	0.72		4.59	2.25		
	21	Kpniz	0.83	0.76	5.10	1.86	4.55	2.82

error (RMSE), and mean absolute gross errors (MAGEs) were calculated. MAGE was used as a measure of mAUHI fitness.

All three models (SL, ML, and MSL) were applied only for the station group A, which gave the highest UHI intensities and CC for oAUHI and oSUHI time series (see Section III-C). The regression model that gave the best results for UHI intensity prediction (lowest MAGE errors) was applied for further analysis for other station groups—B, C, and D. Such an approach allows an analysis of the effectiveness of the proposed methodology in a practical application.

In Sections III-C and III-D, the statistical models were calculated in loops. For the case of a single station, any given model (SL, MSL, or ML) was built using the average directional coefficient and intercept calculated for four remaining stations. The mAUHI errors were calculated for each station using the actual oAUHI. Such an approach gave mAUHI error statistics for all 20 stations grouped into A, B, C, and D (see Tables IV and V).

III. RESULTS

A. Relationship Between AT and MODIS LST

The nature of direct *in-situ* measurements of AT is very different from the satellite remote sensing approach. The relationship between remotely sensed radiative surface temperature

and kinetic AT is even more complex for urban areas especially when the differences in the spatial resolution of satellite observations and source areas for *in-situ* measurements are considered. Nevertheless, surface and ATs are physically related. Passive thermal satellite observations are possible only when the sky is cloudless. Under such conditions, surfaces convectively heat up the air masses above.

Given the characteristics of the *in-situ* stations that were utilized, it is important to prove the relationship between the measured AT and MODIS LST. Fig. 2 shows a scatterplot for the relationship between those two types of temperature, on the basis that only pixels closest to the ground stations were taken into account. A strong, linear, direct relationship between LST and the *in-situ* AT was, therefore, proven (see Fig. 2).

B. Relationship Between oAUHI and oSUHI

Using Hoza station as an urban reference, oAUHI and oSUHI were calculated using all other stations considered as the second item of UHI pair (see Table III). In general case, the AUHI phenomenon becomes less significant with increasing distance from the city center [49]. Here, the distance from the city center was not addressed. The 1-NDVI+ISA was utilized as a primary parameter for the analyses.

We note gradual changes both in the values of CC and oAUHI and oSUHI for all of the stations' groups A, B, C, and D. In each

TABLE IV
RESULTS OF UHI STATISTICAL PREDICTION USING THREE REGRESSION MODELS FOR THE STATION GROUP A

4A. Simple linear regression model (SL)									
	MBE [°C]:	MAGE [°C]:	RMSE [°C]:	CC:	SD(mod)/SD(obs):	intercept	dir. coef.	MAGE/avAUHI [°C]:	MAGE/avAUHI [°C]:
Anton	0.09	1.66	1.99	0.71	0.62	1.69	1.08	0.36	
Powsi	1.33	1.68	2.11	0.69	0.92	1.66	1.17	0.37	
Kobia	1.98	2.11	2.48	0.83	1.13	1.78	1.16	0.46	0.40
Sulej	-0.62	1.55	1.95	0.72	0.76	1.44	1.12	0.34	
Kpniz	-1.76	2.15	2.68	0.83	0.57	1.42	1.01	0.47	
4B. Multiple linear regression model (ML)									
Anton	0.02	1.62	1.94	0.73	0.63	1.13	1.08	0.36	
Powsi	1.32	1.67	2.08	0.71	0.93	1.08	1.17	0.37	
Kobia	1.99	2.11	2.47	0.84	1.15	1.13	1.16	0.46	0.39
Sulej	-0.53	1.52	1.91	0.72	0.76	0.80	1.12	0.33	
Kpniz	-1.48	2.01	2.52	0.81	0.59	0.65	1.01	0.44	
4C. MAGE minimized simple linear regression model (MSL)									
Anton	0.21	1.65	1.99	0.71	0.66	1.69	1.13	0.36	
Powsi	-0.01	1.27	1.57	0.69	0.60	1.66	0.76	0.28	
Kobia	0.04	1.18	1.45	0.83	0.68	1.78	0.70	0.26	0.31
Sulej	-0.12	1.46	1.92	0.72	0.91	1.44	1.35	0.32	
Kpniz	-0.39	1.45	1.92	0.83	0.99	1.42	1.77	0.32	

TABLE V
RESULTS OF UHI STATISTICAL PREDICTION USING MSL FOR STATION GROUPS B, C, AND D

	No.	Station	MBE [°C]:	MAGE [°C]:	RMSE [°C]:	CC:	SD(mod)/SD(obs):	intercept	direction coef.	MAGE/avUHI [°C]	MAGE/avUHI [°C]
Group D (urban stations)	2	Orzyc	0.03	0.59	0.80	0.46	0.21	1.02	0.26	0.43	
	3	Kamio	0.03	0.93	1.20	0.37	0.39	0.99	0.45	0.67	
	4	Olbra	0.12	0.67	0.88	0.47	0.35	1.02	0.42	0.48	0.54
	5	Bokse	-0.33	0.79	1.13	0.44	0.33	0.94	0.47	0.57	
	6	Zgrzm	-0.09	0.76	1.00	0.62	0.67	0.95	0.84	0.55	
Group C (sub-urban 1)	7	Liman	0.08	0.84	1.06	0.57	0.45	1.43	0.46	0.37	
	8	Conra	0.26	0.98	1.20	0.59	0.45	1.46	0.56	0.44	
	9	Włoda	0.03	1.02	1.29	0.54	0.48	1.4	0.83	0.45	0.47
	10	Kamin	-0.54	1.36	1.77	0.49	0.52	1.27	0.69	0.61	
	11	Zielo	-0.02	1.05	1.35	0.78	0.83	1.36	1.11	0.47	
Group B (sub-urban 2)	12	Micha	-0.5	1.62	2.19	0.66	1.1	1.28	1.64	0.43	
	13	Berna	-0.24	1.30	1.66	0.59	0.72	1.51	1.06	0.34	
	14	Legio	-0.02	1.19	1.55	0.62	0.66	1.58	0.79	0.31	0.38
	15	Lomia	0.28	1.58	1.92	0.72	0.49	1.87	0.56	0.42	
	16	Thusz	0.19	1.58	1.95	0.73	0.57	1.79	0.64	0.42	

case, the intensity of oAUHI is higher than of oSUHI, which is probably connected with the differences in source areas for AT and LST measurements.

The gradual increase in oAUHI and oSUHI intensities is accompanied by a gradual increase in the CC values, which describe the strength of the linear relationship between oAUHI and oSUHI. In general, the less urbanized the surroundings of the second item of UHI pair are, the higher the oAUHI and oSUHI values are.

The most apparent (as compared to other groups) differences in the thermal characteristics between Hoza and group A imply the highest oSUHI and oAUHI values for such pair. Artificial urban surfaces have higher thermal inertia than surrounding natural or seminatural areas. Moreover, natural areas are abundant with vegetation, which increases absolute humidity. Hence,

the cooling rate of the natural areas is much higher than of the urbanized areas, which can cause near-ground AT inversion after sunset (cooler air masses are beneath warmer masses). Such a process is most apparent when there is no cloud cover—and only in such conditions, satellite measurements of LST are possible. This explains the highest oAUHI and oSUHI values for group A and Hoza location. Consequently, CC observed for this pair is also the highest.

When Tables II and III are considered, it can be noted that the changes in the z0 and SVF values are not proportional to gradual changes in the CC of the AUHI/SUHI relationship. The z0 parameter was based on DSM data, which included vegetation, therefore it has high values both for built-up stations (Hoza) and those surrounded with trees (Kpniz). This also explains no direct relationship between oSUHI and oAUHI and SVF.

Relationship between LST and AT for all stations (years 2008-17)

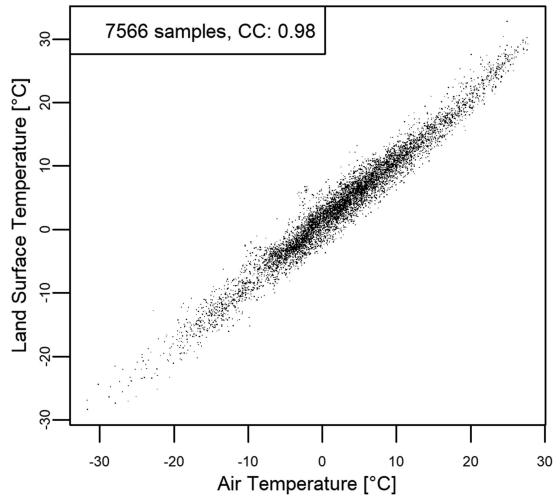


Fig. 2. Relationship between air and surface temperatures for all available data samples.

LCZs are one of the most comprehensive classification frameworks for urban areas [53]. However, the delimitation of specific classes across the city is a challenge itself [54], [55]. Moreover, thermal contrasts within single classes are documented [56]. In spite of the fact that we note significant differences in “UA urban,” “UA rural,” NDVI and ISA values (see Table II), and oSUHI and oAUHI values (see Table III) for the stations Wloda, Kamin, Kamio, Bokse, and Orzyc, they were all assigned to the same class LCZ 5. This might hamper quantitative analyses, therefore, we prioritized the 1-NDVI-ISA parameter for grouping the locations of the *in-situ* stations.

C. Statistical Prediction of UHI Intensity—Choice of a Regression Model Based on Error Analysis

Based on the calculated errors, CC and the ratio between the standard deviation of mAUHI and oAUHI (SD ratio), we evaluated the modeling results (see Table IV). The closer to 1 the SD ratio is, the lower the errors and the higher CC are, and the modeling results were considered better. In each case, the SL, the ML, and the MSL underestimated AUHI values in the case of station Kpniz and Sulej and overestimated in case of Kobia and Anton. The SL gave MAGE in a range from 1.55 to 2.15 °C, referred to as 0.34–0.47 °C of the average AUHI intensity noted for group A (MAGE/avAUHI ratio) [see Table IV(A)].

The same CC value (0.83) was observed for both Kobia and Kpniz stations and the MBE values were very different for those stations: 1.98 and –1.76 °C, whereas RMSE values were similar: 2.48 and 2.68 °C accordingly. Moreover, MAGE was very similar: 2.11 and 2.15 °C. Powisi has the value of the ratio between the standard deviation of mAUHI and oAUHI closest to 1.

The ML gave slightly better modeling results in terms of MBE and MAGE and RMSE [see Table IV(B)]. The values of CC, SD ratio, or MAGE/avAUHI ratio have the same or very similar values. ML changes the directional coefficient and the intercept of the regression line in comparison to the SL, but

the difference is not significant within two decimal places (see Table IV).

When the iterative procedure is applied (MSL), the prediction results are much better compared to SLs and MLs [see Table IV(C)]. The minimization of MAGE improves the results in almost every aspect, namely MBE (except Anton station), RMSE (except Anton and Sulej), and SD ratio (except Powisi and Kobia). The MAGE/avAUHI ratio was also improved when the MSL was used—it had the range between 0.28 and 0.36 °C. Interestingly, all utilized regression models gave very similar modeling results for Anton station.

The improvements obtained by the ML compared to the SL are neglectable. Given the fact that the ML requires additional data (NDVI time series) and that the MSL gave the best modeling results, we chose the MSL for further analyses.

To maintain the brevity of this article, the MSL results for station group A are only presented in Table IV.

D. Statistical Prediction of UHI Intensity for Station Groups B, C, and D

In general, increasing urbanization of *in-situ* locations considered as the second item of UHI pair causes approximately directly proportional decrease in mAUHI errors (see Table V). Group A [see Table IV(C)], which has the 1-NVDI+ISA values below 0.50 (see Table II), gave the highest errors as compared to group B (1-NVDI+ISA range: 0.50–0.70), C (1-NVDI+ISA range: 0.70–0.90), and D (1-NVDI+ISA range: 0.90–1.10). Lower error values in groups B, C, and D do not indicate a better MSL performance—it can be easily explained by lower AUHI intensities obtained in those groups (see Table III). This is confirmed by the MAGE/avAUHI ratio (see Table V), which is the lowest for group A, higher for groups C and B, and the highest for group D.

To better assess the ability of the MSL to reproduce AUHI intensity, we prepared a set of scatterplots presenting the relationship between mAUHI and oAUHI for the station, for which the MAGE error was the lowest (see Fig. 3).

It can be noted that the scatterplots presented in Fig. 3 are compliant with findings based on Table V. The MSL calculated for the Kobia station (group A) gave the highest values of R^2 (coefficient of determination) and CC. In this case, there are few outlying points, but their overall scatterplot indicates a decent MSL performance.

However, when the degree of urbanization was increased (stations Legio, Liman, and Orzyc), the modeling results were worsened. The number of outliers was increased and the point clouds were not aligned with the regression line. This is confirmed by much lower values of R^2 and CC.

IV. DISCUSSION

A. Comments on the Obtained UHI Intensities in Light of Previous Works Conducted for the City of Warsaw

The previous studies that investigate Warsaw’ SUHI intensity that used a comparable sensor, in terms of its spatial resolution, are very scarce. Using the “urban-other” indicator [51], Gawuc [57] documented a nighttime SUHI intensity of 2.1 °C using a

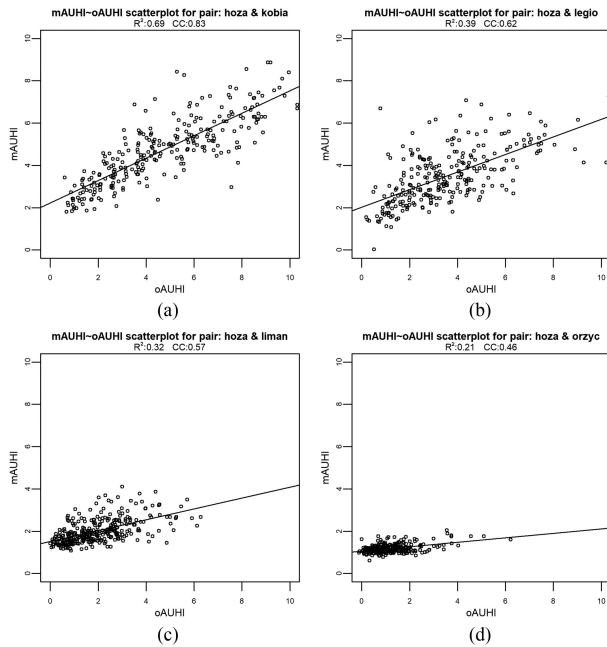


Fig. 3. Scatterplots of the mAUHI/oAUHI relationship.

single MODIS image. Temporal composites were a subject of the latest study for the city of Warsaw [14]. 15-year mean SUHI intensity based on LST temporal composition was documented of at least 1 °C. Such values are in line with our results.

The previous investigations, based on AT daily minimum values (which may occur not at the same time on the analyzed posts), have shown that AUHI in the center of Warsaw compared to Chopin Airport meteorological station in the years 2011–2012 was of 1 °C stronger and of a bigger spatial extent than in the years 2001–2002. In 2011–2012, yearly average AUHI reached 2.5 °C in the city center, but in chosen days, it reached 10 °C [50], [58], however, it concerned the differences between the lowest 1-h means noted at the given station and airport station.

The other analysis of daily AT minimum values (the lowest hourly mean of 24 h—which in general presents nighttime AUHI) in the years 2008–2014 has shown 3.0 °C yearly mean difference between city center and suburban areas (Kobia and Powsi) and over 3.5 °C between the city center and forest clearing (Kpniz) outside Warsaw [59].

In this study, the oAUHI was, in general, of higher values (see Table III), mainly because of different method to calculate oAUHI intensity. Minimum daily AT usually occurs in the early morning, but not always. Sometimes under low air pressure systems or in frontal zones moving over Warsaw the minimum AT may occur at completely different hours. In the current study, oAUHI was based on 10-min averages of AT and calculated in a point-by-point manner for all of the stations at the same moment. This is the main reason why mean yearly oAUHI in the years 2008–2017 reached 5.1 °C (Hoza-Kpniz). Moreover, as the overall degree of urbanization and imperviousness have increased in the city of Warsaw, we anticipate that the mean background urban AT might have risen as well. It would make sense, since neither the closest surroundings of the measuring points nor SVFs have changed in the analyzed period. However,

to confirm this, additional studies would be necessary, what exceeds the scope of this article.

B. Documented AUHI and SUHI Investigations by Means of the Simultaneous Ground and Remote Sensing Data

Sheng *et al.* [30] concluded that AUHI and SUHI intensities are very different and cannot be compared. This might be caused by the fact that they used specific UHI indicators [53], namely “magnitude,” “range,” “urban–rural,” and “urban–agriculture.” Those indicators must be considered as a different approach for UHI quantification as compared to our approach. We used direct measures of UHI estimation, namely “temperature at urban point minus temperature at rural point” subtraction. This allowed for a consistent analysis of the AUHI/SUHI relationship. Sun *et al.* [60] documented low differences between simultaneous AUHI and SUHI (“2 K predominantly”). The majority of the obtained MAGE errors in our study are comparable to or lower than 2 °C (see Tables IV and V). However, as the AT in [60] was not measured directly, their results are not directly comparable. The equation is given by Zhang [34] that binds AUHI with the product of $1/a \cdot \text{SUHI}$ is basically a form of a simplified linear regression model. This equation assumes that AUHI and SUHI have always a linear relationship. This—as presented in our study—is not fully true, because decent results of mAUHI were only obtained for specific station pairs, namely those with the highest urban–rural contrast in terms of urbanization (Hoza and station group A). Therefore, we comment that the equation given by Zhang *et al.* [34] is true in specific cases, but it is oversimplified in general case.

One of our findings is that the urbanization has an apparent and approximately directly proportional impact on the relationship between oAUHI and oSUHI. Such a conclusion seems very logical since the highest oAUHI and oSUHI intensities are observed when the “urban–rural” pair consists of the most urbanized urban station and the least urbanized the second item of UHI pair. This is consistent with the previous study of the impact of rural stations’ locations on AUHI intensities [39], [40]. The problem of choosing the rural reference is also commented on in [37]. Moreover, Montávez *et al.* [61] found that the greater the difference between urban and rural thermal admittances, the greater the UHI intensity. These findings are in line with ours.

C. Modeling of AUHI Using Other Methods—Comparison of Models Efficiency

We can anticipate that our modeling approach is acceptable only in those cases when error statistics (along with R^2 and CC noted between mAUHI and oAUHI) are comparable with similar studies. However, UHI investigations that utilize simultaneous ground and remotely sensed observations are not frequent. Referring to the literature is difficult given the fact that utilizing simultaneous ground and remote sensing observations limits the analyses for the satellite overpasses. Moreover, the overpass times of Terra and Aqua are not equivalent to the moment when the maximum AUHI or SUHI typically occurs (in the afternoon). Nevertheless, we compare our results with previously documented to draw a background for the final conclusions.

Theeuwes *et al.* [39] obtained the R^2 coefficient between the modeled and observed AUHI (their Fig. 7) equal 0.65, which is comparable with R^2 presented in Fig. 3(a) (0.69) calculated for the station Kobia. However, corresponding RMSE in this study (1.45 °C—Table IV) is slightly higher than the one documented in [39]—0.91 °C. It is important to comment that the diagnostic equation proposed in the mentioned study is much more complex as it takes into account many more parameters than the MSL, which is based on AT and LST observations solely. The statistical models based on several parameters were able to explain 75% of the AUHI variance in the study of [37] and in 85% in the study of [41]. Results presented here are comparable, yet slightly worse or moderately worse. In contrast, the R^2 coefficient obtained in [38] explained 42% of the AUHI variance, whereas R^2 obtained here was higher in case of Kobia station [0.69—Fig. 3(a)] and comparable to R^2 for Legio station [0.39—Fig. 3(b)]. However, the analyses presented in [38] were not limited to satellite overpass time, which limits comparison with our results. In the study of [6], Bottyán and Unger were able to effectively (errors lower than 0.2 °C were obtained for 57% of city area) predict AUHI intensity. Even though, in the current study, each station group represents a different area of the city, a precise comparison of [6] findings with ours would exceed the scope of the current article. However, since the lowest modeling errors obtained were of higher values (MAGE = 1.18 °C and RMSE = 1.45 °C for Kobia station—Table IV), we can comment that the more sophisticated model of [6] using much more input parameters provided better modeling results. On the other hand, in the study of Hjort *et al.* [62], the simpler model (generalized linear model) gave better results than the more complex model (boosted regression tree). In [63], thermal satellite data are used for nonurban AT prediction, but the obtained model errors (0.9–1.4 °C) are comparable to those of our study. The documented R^2 equals 0.84 in [32] is higher than presented here, however, Majkowska *et al.* [32] used Landsat 5 LST data for prediction of urban AT, not AUHI intensity—similarly to [62].

Considering the literature review, we conclude that satisfactory results were obtained only for AUHI measured by the “urban–rural” station pairs, which consist of the stations with the highest difference in urbanization. In the case of our study, this is the stations’ group A, which is utilized as the second item UHI pair along with the Hoza station as an urban reference (first item). The proposed methodology gave worse results for the stations’ group B and significantly worse for the groups C and D.

To sum up, underlining the limitations of our methodology is necessary. First, as it was based on instantaneous remote sensing data collected with sun-synchronous platforms, its practical application is limited to the time of day comparable to the moments of satellites overpasses (00:30–1:30 UTC and 20:00–20:50 UTC). Second, the proposed regression model should be applied along with satellite imagery of similar spatial resolution as MODIS. Data from other satellites might give erroneous results. Third, as we did not include temporal analysis, it is unknown if there should be any restrictions in applying the model in certain synoptic conditions. Finally, it should be noted that

any linear regression model (regardless of the method to obtain necessary coefficients) is an oversimplification of AUHI–SUHI relationship. The presented methodology is not fit for detailed local-scale UHI analyses. It can only provide an approximation of AUHI intensity. Hence, the current form of the proposed method must be used with care.

D. Potential for Further Analyses

We can speculate that a more complex regression model based on oSUHI might be a more efficient tool for AUHI prediction. However, to build such model, a much more extensive analysis would be needed. First of all, more remote sensing data from different platforms should be considered. Thermal satellite data with a higher spatial resolution than MODIS might bring a more distinctive approximation of thermal environment in specific urban locations. There are several sensors, which could provide appropriate data (Landsat, VIIRS, ECOSTRESS, ASTER, etc.). Airborne thermal measurements might be helpful as well. Such data could help to understand better the urban LST–AT and SUHI–AUHI relationships. However, it would be costly and extremely difficult to obtain such material for Warsaw or similar cities due to its cloudiness conditions. Also, much more ancillary LU/LC data would be necessary. Second of all, to extract deeper insights from much larger datasets, one would need to apply much more sophisticated statistical analyses.

In this study, there was no seasonal analysis presented. It would provide a more in-depth insight into the statistical models’ performance. Nevertheless, the study aimed to analyze if there is a potential of the oAUHI/oSUHI relationship for robust statistical modeling. It was proved that there is provided that certain conditions regarding the station pairs are fulfilled and that the limitations of the method are understood. However, a seasonal analysis and application for other cities must be done in the following publication, which is planned in the future.

Given the fact that wind speed has an apparent impact on AUHI [2] utilization of this parameter might have been important in the analysis of AUHI/SUHI relationship. However, such data are not registered along with AT on the stations maintained by the Polish Academy of Sciences. As the goal of our approach was to limit the number of input data, we used only AT, LST, and NDVI measurements. ISA was collected free of charge from Copernicus Services. Using those observations only was sufficient to fulfill the objective of the presented research.

The proposed MSL is based on an iteration to minimize MAGE errors. It can be noted that such an iterative procedure would not be possible for the city with no *in-situ* observational network. However, before applying the presented methodology for the cities with no ground measurements available, the statistical model should be calibrated by means of an existing *in-situ* network in similar urban environments. Nevertheless, the developed methodology can be applied in other cities for an approximated AUHI estimation. However, its effectiveness of such transfer must be analyzed in the following publication. This exceeds the scope of the presented investigation.

V. SUMMARY AND CONCLUSION

In this article, the relationship between nocturnal SUHI and AUHI was applied as a basis for the statistical modeling of AUHI. The data were collected over 10 years (2008–2017). The set of 442 MODIS images acquired at a maximum of 35° off-nadir were selected for the periods of low cloudiness. *In-situ* observations were collected for the exact time of the satellites overpasses, using 21 automatic stations located in various locations across the city covering different micrometeorological environments.

Our results showed that the relationship between oSUHI and oAUHI is strongly dependent on surface imperviousness (ISA) and vegetation cover (given by NDVI), moderately dependent on the Urban Atlas classes or LCZs and weakly dependent on the SVF and roughness length for momentum. The strongest linear relationship between simultaneous oSUHI and oAUHI was noted for those “urban–rural” station pairs, whose surroundings have the highest differences in urbanization, and the highest simultaneous oSUHI and oAUHI intensities observed. The oSUHI/oAUHI linear relationship decreases gradually with the increasing urbanization of the surroundings of the stations considered as the second item of UHI pair.

Three modeling approaches were compared and simple linear regression based on iterative minimization of the MAGE errors was utilized for prediction of mAUHI for all of the stations in all groups. The minimal MAGE errors for each group were obtained for stations: group A: Kobia (1.18 °C), group B: Legio (1.19 °C), group C: Liman (0.84 °C), and group D: Orzyc (0.59 °C). The ratio between group average MAGE of mAUHI and group average oAUHI was lowest (0.31 °C) for the stations group with the least urbanized surroundings (group A) and it is approximately directly proportional with increasing urbanization of the surroundings of the stations considered as the second item of UHI pair (0.38 °C—group B, 0.47 °C—group C, and 0.54 °C—group D). We conclude that the simple regression model (with the iterative procedure for minimization of MAGE) describing the oAUHI and oSUHI relationship is capable of providing satisfactory results for the approximated prediction of nighttime AUHI. However, the statistical model must be built using the station pairs with the highest differences in urbanization possible.

Our methodology, as an alternative for more complex approaches, might be useful for an approximate AUHI estimation for the cities with no AT observing network. Further work is planned to generalize the presented methodology for other cities including seasonal analysis of the statistical model performance.

REFERENCES

- [1] T. R. Oke, “The energetic basis of the urban heat island,” *Q. J. Roy. Meteorol. Soc.*, vol. 108, no. 455, pp. 1–24, Jan. 1982, doi: [10.1002/qj.49710845502](https://doi.org/10.1002/qj.49710845502).
- [2] T. R. Oke, “The heat island of the urban boundary layer: Characteristics, causes and effects,” in *Wind Climate in Cities*, J. E. Cermak, A. G. Davenport, E. J. Plate, and D. X. Viegas, Eds. Dordrecht, The Netherlands: Springer, 1995, pp. 81–107.
- [3] P. I. Figuerola and N. A. Mazzeo, “Urban-rural temperature differences in Buenos Aires,” *Int. J. Climatol.*, vol. 18, no. 15, pp. 1709–1723, Dec. 1998, doi: [10.1002/\(SICI\)1097-0088\(199812\)18:15<1709::AID-JOC338>3.0.CO;2-I](https://doi.org/10.1002/(SICI)1097-0088(199812)18:15<1709::AID-JOC338>3.0.CO;2-I).
- [4] Y.-H. Kim and J.-J. Baik, “Spatial and temporal structure of the urban heat island in Seoul,” *J. Appl. Meteorol.*, vol. 44, no. 5, pp. 591–605, May 2005, doi: [10.1175/JAM2226.1](https://doi.org/10.1175/JAM2226.1).
- [5] L. W. A. van Hove, C. M. J. Jacobs, B. G. Heusinkveld, J. A. Elbers, B. L. van Driel, and A. A. M. Holtslag, “Temporal and spatial variability of urban heat island and thermal comfort within the Rotterdam agglomeration,” *Building Environ.*, vol. 83, pp. 91–103, Jan. 2015, doi: [10.1016/j.buildenv.2014.08.029](https://doi.org/10.1016/j.buildenv.2014.08.029).
- [6] Z. Bottyán and J. Unger, “A multiple linear statistical model for estimating the mean maximum urban heat island,” *Theor. Appl. Climatol.*, vol. 75, no. 3, pp. 233–243, Sep. 2003, doi: [10.1007/s00704-003-0735-7](https://doi.org/10.1007/s00704-003-0735-7).
- [7] D. J. Murphy, M. H. Hall, C. A. S. Hall, G. M. Heisler, S. V. Stehman, and C. Anselmi-Molina, “The relationship between land cover and the urban heat island in northeastern Puerto Rico,” *Int. J. Climatol.*, vol. 31, no. 8, pp. 1222–1239, Jun. 2011, doi: [10.1002/joc.2145](https://doi.org/10.1002/joc.2145).
- [8] T. R. Oke, in *Initial Guidance to Obtain Representative Meteorological Observations at Urban Sites*. Geneva, Switzerland: World Meteorol. Org., 2006.
- [9] I. D. Stewart, “A systematic review and scientific critique of methodology in modern urban heat island literature,” *Int. J. Climatol.*, vol. 31, no. 2, pp. 200–217, Feb. 2011, doi: [10.1002/joc.2141](https://doi.org/10.1002/joc.2141).
- [10] J. A. Voogt and T. R. Oke, “Thermal remote sensing of urban climates,” *Remote Sens. Environ.*, vol. 86, no. 3, pp. 370–384, Aug. 2003, doi: [10.1016/S0034-4257\(03\)00079-8](https://doi.org/10.1016/S0034-4257(03)00079-8).
- [11] J. A. Sobrino, R. Oltra-Carrió, G. Sòria, R. Bianchi, and M. Paganini, “Impact of spatial resolution and satellite overpass time on evaluation of the surface urban heat island effects,” *Remote Sens. Environ.*, vol. 117, pp. 50–56, Feb. 2012, doi: [10.1016/j.rse.2011.04.042](https://doi.org/10.1016/j.rse.2011.04.042).
- [12] L. Hu, A. Monaghan, J. A. Voogt, and M. Barlage, “A first satellite-based observational assessment of urban thermal anisotropy,” *Remote Sens. Environ.*, vol. 181, pp. 111–121, Aug. 2016, doi: [10.1016/j.rse.2016.03.043](https://doi.org/10.1016/j.rse.2016.03.043).
- [13] D. M. Stoms, M. J. Bueno, and F. W. Davis, “Viewing geometry of AVHRR image composites derived using multiple criteria,” *Photogramm. Eng. Remote Sens.*, vol. 63, pp. 681–689, 1997.
- [14] L. Gawuc and J. Struzewska, “Impact of MODIS quality control on temporally aggregated urban surface temperature and long-term surface urban heat island intensity,” *Remote Sens.*, vol. 8, no. 5, pp. 374, May 2016, doi: [10.3390/rs8050374](https://doi.org/10.3390/rs8050374).
- [15] L. Hu and N. A. Brunzell, “The impact of temporal aggregation of land surface temperature data for surface urban heat island (SUHI) monitoring,” *Remote Sens. Environ.*, vol. 134, pp. 162–174, Jul. 2013, doi: [10.1016/j.rse.2013.02.022](https://doi.org/10.1016/j.rse.2013.02.022).
- [16] P. Wu, H. Shen, L. Zhang, and F.-M. Göttsche, “Integrated fusion of multi-scale polar-orbiting and geostationary satellite observations for the mapping of high spatial and temporal resolution land surface temperature,” *Remote Sens. Environ.*, vol. 156, pp. 169–181, Jan. 2015, doi: [10.1016/j.rse.2014.09.013](https://doi.org/10.1016/j.rse.2014.09.013).
- [17] B. Dousset and F. Gourmelon, “Satellite multi-sensor data analysis of urban surface temperatures and landcover,” *ISPRS J. Photogramm. Remote Sens.*, vol. 58, no. 1/2, pp. 43–54, 2003, doi: [10.1016/S0924-2716\(03\)00016-9](https://doi.org/10.1016/S0924-2716(03)00016-9).
- [18] J. P. Walawender, M. Szymanowski, M. J. Hajto, and A. Bokwa, “Land surface temperature patterns in the urban agglomeration of Krakow (Poland) derived from Landsat-7/ETM+ data,” *Pure Appl. Geophys.*, vol. 171, no. 6, pp. 913–940, Jun. 2014, doi: [10.1007/s00024-013-0685-7](https://doi.org/10.1007/s00024-013-0685-7).
- [19] N. Chrysoulakis, “Estimation of the all-wave urban surface radiation balance by use of ASTER multispectral imagery and *in situ* spatial data,” *J. Geophys. Res.*, vol. 108, no. D18, pp. 4582, Sep. 2003, doi: [10.1029/2003JD003396](https://doi.org/10.1029/2003JD003396).
- [20] S. Kato and Y. Yamaguchi, “Analysis of urban heat-island effect using ASTER and ETM+ Data: Separation of anthropogenic heat discharge and natural heat radiation from sensible heat flux,” *Remote Sens. Environ.*, vol. 99, no. 1/2, pp. 44–54, Nov. 2005, doi: [10.1016/j.rse.2005.04.026](https://doi.org/10.1016/j.rse.2005.04.026).
- [21] M. S. Wong, J. Yang, J. Nichol, Q. Weng, M. Menenti, and P. Chan, “Modeling of anthropogenic heat flux using HJ-1B Chinese small satellite image: A study of heterogeneous urbanized areas in Hong Kong,” *IEEE Geosci. Remote Sens. Lett.*, vol. 12, no. 7, pp. 1466–1470, Jul. 2015, doi: [10.1109/LGRS.2015.2409111](https://doi.org/10.1109/LGRS.2015.2409111).
- [22] A. Buyantuyev and J. Wu, “Urban heat islands and landscape heterogeneity: Linking spatiotemporal variations in surface temperatures to land-cover and socioeconomic patterns,” *Landscape Ecol.*, vol. 25, no. 1, pp. 17–33, Sep. 2009, doi: [10.1007/s10980-009-9402-4](https://doi.org/10.1007/s10980-009-9402-4).

- [23] G. Huang, W. Zhou, and M. L. Cadenasso, "Is everyone hot in the city? Spatial pattern of land surface temperatures, land cover and neighborhood socioeconomic characteristics in Baltimore, MD," *J. Environ. Manage.*, vol. 92, no. 7, pp. 1753–1759, Jul. 2011, doi: [10.1016/j.jenvman.2011.02.006](https://doi.org/10.1016/j.jenvman.2011.02.006).
- [24] G. D. Jenerette, S. L. Harlan, A. Brazel, N. Jones, L. Larsen, and W. L. Stefanov, "Regional relationships between surface temperature, vegetation, and human settlement in a rapidly urbanizing ecosystem," *Landscape Ecol.*, vol. 22, no. 3, pp. 353–365, Dec. 2006, doi: [10.1007/s10980-006-9032-z](https://doi.org/10.1007/s10980-006-9032-z).
- [25] M. Demuzere *et al.*, "Mitigating and adapting to climate change: Multi-functional and multi-scale assessment of green urban infrastructure," *J. Environ. Manage.*, vol. 146, pp. 107–115, Dec. 2014, doi: [10.1016/j.jenvman.2014.07.025](https://doi.org/10.1016/j.jenvman.2014.07.025).
- [26] J. Tan *et al.*, "The urban heat island and its impact on heat waves and human health in Shanghai," *Int. J. Biometeorol.*, vol. 54, no. 1, pp. 75–84, Jan. 2010, doi: [10.1007/s00484-009-0256-x](https://doi.org/10.1007/s00484-009-0256-x).
- [27] Y. Wang, U. Berardi, and H. Akbari, "Comparing the effects of urban heat island mitigation strategies for Toronto, Canada," *Energy Buildings*, vol. 114, pp. 2–19, Feb. 2016, doi: [10.1016/j.enbuild.2015.06.046](https://doi.org/10.1016/j.enbuild.2015.06.046).
- [28] J. E. Nichol and M. S. Wong, "Spatial variability of air temperature and appropriate resolution for satellite-derived air temperature estimation," *Int. J. Remote Sens.*, vol. 29, no. 24, pp. 7213–7223, Dec. 2008, doi: [10.1080/01431160802192178](https://doi.org/10.1080/01431160802192178).
- [29] J. E. Nichol, W. Y. Fung, K. Lam, and M. S. Wong, "Urban heat island diagnosis using ASTER satellite images and 'in situ' air temperature," *Atmos. Res.*, vol. 94, no. 2, pp. 276–284, Oct. 2009, doi: [10.1016/j.atmosres.2009.06.011](https://doi.org/10.1016/j.atmosres.2009.06.011).
- [30] L. Sheng, X. Tang, H. You, Q. Gu, and H. Hu, "Comparison of the urban heat island intensity quantified by using air temperature and Landsat land surface temperature in Hangzhou, China," *Ecol. Indicators*, vol. 72, pp. 738–746, Jan. 2017, doi: [10.1016/j.ecolind.2016.09.009](https://doi.org/10.1016/j.ecolind.2016.09.009).
- [31] N. Schwarz, U. Schlink, U. Franck, and K. Großmann, "Relationship of land surface and air temperatures and its implications for quantifying urban heat island indicators—An application for the city of Leipzig (Germany)," *Ecol. Indicators*, vol. 18, pp. 693–704, Jul. 2012, doi: [10.1016/j.ecolind.2012.01.001](https://doi.org/10.1016/j.ecolind.2012.01.001).
- [32] A. Majkowska, L. Kolendowicz, M. Półrolniczak, J. Hauke, and B. Czernecki, "The urban heat island in the city of Poznań as derived from Landsat 5 TM," *Theor. Appl. Climatol.*, vol. 128, no. 3/4, pp. 769–783, May 2017, doi: [10.1007/s00704-016-1737-6](https://doi.org/10.1007/s00704-016-1737-6).
- [33] J. A. Azevedo, L. Chapman, and C. L. Muller, "Quantifying the daytime and night-time urban heat island in Birmingham, UK: A comparison of satellite derived land surface temperature and high resolution air temperature observations," *Remote Sens.*, vol. 8, no. 2, Feb. 2016, Art. no. 153, doi: [10.3390/rs8020153](https://doi.org/10.3390/rs8020153).
- [34] F. Zhang, X. Cai, and J. E. Thornes, "Birmingham's air and surface urban heat islands associated with Lamb weather types and cloudless anticyclonic conditions," *Prog. Phys. Geogr., Earth Environ.*, vol. 38, no. 4, pp. 431–447, Aug. 2014, doi: [10.1177/0309133314538725](https://doi.org/10.1177/0309133314538725).
- [35] T. R. Oke, "City size and the urban heat island," *Atmos. Environ. (1967)*, vol. 7, no. 8, pp. 769–779, Aug. 1973, doi: [10.1016/0004-6981\(73\)90140-6](https://doi.org/10.1016/0004-6981(73)90140-6).
- [36] T. R. Oke, "Canyon geometry and the nocturnal urban heat island: Comparison of scale model and field observations," *J. Climatol.*, vol. 1, no. 3, pp. 237–254, 1981, doi: [10.1002/joc.3370010304](https://doi.org/10.1002/joc.3370010304).
- [37] T. Brandsma and D. Wolters, "Measurement and statistical modeling of the urban heat island of the city of Utrecht (The Netherlands)," *J. Appl. Meteorol. Climatol.*, vol. 51, no. 6, pp. 1046–1060, Feb. 2012, doi: [10.1175/JAMC-D-11-0206.1](https://doi.org/10.1175/JAMC-D-11-0206.1).
- [38] P. Hoffmann, O. Krueger, and K. H. Schlünzen, "A statistical model for the urban heat island and its application to a climate change scenario," *Int. J. Climatol.*, vol. 32, no. 8, pp. 1238–1248, Jun. 2012, doi: [10.1002/joc.2348](https://doi.org/10.1002/joc.2348).
- [39] N. E. Theeuwes, G.-J. Steeneveld, R. J. Ronda, and A. A. M. Holtslag, "A diagnostic equation for the daily maximum urban heat island effect for cities in northwestern Europe," *Int. J. Climatol.*, vol. 37, no. 1, pp. 443–454, 2017, doi: [10.1002/joc.4717](https://doi.org/10.1002/joc.4717).
- [40] X. Zhang, G.-J. Steeneveld, D. Zhou, C. Duan, and A. A. M. Holtslag, "A diagnostic equation for the maximum urban heat island effect of a typical Chinese city: A case study for Xi'an," *Building Environ.*, vol. 158, pp. 39–50, Jul. 2019, doi: [10.1016/j.buildenv.2019.05.004](https://doi.org/10.1016/j.buildenv.2019.05.004).
- [41] A. Straub *et al.*, "Statistical modelling of spatial patterns of the urban heat island intensity in the urban environment of Augsburg, Germany," *Urban Climate*, vol. 29, Sep. 2019, Art. no. 100491, doi: [10.1016/j.uclim.2019.100491](https://doi.org/10.1016/j.uclim.2019.100491).
- [42] C. I. Anderson, W. A. Gough, and T. Mohsin, "Characterization of the urban heat island at Toronto: Revisiting the choice of rural sites using a measure of day-to-day variation," *Urban Climate*, vol. 25, pp. 187–195, Sep. 2018, doi: [10.1016/j.uclim.2018.07.002](https://doi.org/10.1016/j.uclim.2018.07.002).
- [43] T. Mohsin and W. A. Gough, "Characterization and estimation of urban heat island at Toronto: Impact of the choice of rural sites," *Theor. Appl. Climatol.*, vol. 108, no. 1, pp. 105–117, Apr. 2012, doi: [10.1007/s00704-011-0516-7](https://doi.org/10.1007/s00704-011-0516-7).
- [44] "Strategic conceptions of conditions and directions of spatial development of Warsaw with changes, Legal act LXII/1667/2018, March 1, 2018," Council of Warsaw, 2018.
- [45] K. Błażejczyk *et al.*, "Urban heat island and bioclimatic comfort in Warsaw," in *Counteracting Urban Heat Island Effects in a Global Climate Change Scenario*, F. Musco, Ed. Cham, Switzerland: Springer, 2016, pp. 305–321.
- [46] K. Błażejczyk, M. Kuchcik, A. Błażejczyk, P. Milewski, and J. Szmyd, "Assessment of urban thermal stress by UTCI—Experimental and modelling studies: An example from Poland," *DIE ERDE*, vol. 145, no. 1/2, pp. 16–33, Sep. 2014, doi: [10.12854/erde-145-3](https://doi.org/10.12854/erde-145-3).
- [47] M. Kuchcik, W. Dudek, K. Błażejczyk, P. Milewski, and A. Błażejczyk, "Two faces to the greenery on housing estates—mitigating climate but aggravating allergy. A Warsaw case study," *Urban Forestry Urban Greening*, vol. 16, pp. 170–181, Jan. 2016, doi: [10.1016/j.ufug.2016.02.012](https://doi.org/10.1016/j.ufug.2016.02.012).
- [48] B. Szulczewska *et al.*, "How much green is needed for a vital neighbourhood? In search for empirical evidence," *Land Use Policy*, vol. 38, pp. 330–345, May 2014, doi: [10.1016/j.landusepol.2013.11.006](https://doi.org/10.1016/j.landusepol.2013.11.006).
- [49] M. Kuchcik and P. Milewski, "Urban heat island in Warsaw – an attempt at assessment with the use of Local Climate Zones method," *Acta Geographica Lodziana*, vol. 104, pp. 21–33, 2016.
- [50] K. Błażejczyk *et al.*, *Urban Heat Island in Warsaw. Climate and Urban Conditions*. Warsaw, Poland: Academic Pub., 2014. [Online]. Available: http://rcin.org.pl/Content/56055/WA51_74963_r2014_Miejska-wyspa-ciepla.pdf
- [51] N. Schwarz, S. Lautenbach, and R. Seppelt, "Exploring indicators for quantifying surface urban heat islands of European cities with MODIS land surface temperatures," *Remote Sens. Environ.*, vol. 115, no. 12, pp. 3175–3186, Dec. 2011, doi: [10.1016/j.rse.2011.07.003](https://doi.org/10.1016/j.rse.2011.07.003).
- [52] C. S. B. Grimmond and T. R. Oke, "Aerodynamic properties of urban areas derived from analysis of surface form," *J. Appl. Meteorol.*, vol. 38, no. 9, pp. 1262–1292, Sep. 1999, doi: [10.1175/1520-0450\(1999\)038<1262:APOUAD>2.0.CO;2](https://doi.org/10.1175/1520-0450(1999)038<1262:APOUAD>2.0.CO;2).
- [53] I. D. Stewart and T. R. Oke, "Local climate zones for urban temperature studies," *Bull. Amer. Meteorol. Soc.*, vol. 93, no. 12, pp. 1879–1900, May 2012, doi: [10.1175/BAMS-D-11-00019.1](https://doi.org/10.1175/BAMS-D-11-00019.1).
- [54] B. Bechtel *et al.*, "Generating WUDAPT level 0 data – Current status of production and evaluation," *Urban Climate*, vol. 27, pp. 24–45, Mar. 2019, doi: [10.1016/j.uclim.2018.10.001](https://doi.org/10.1016/j.uclim.2018.10.001).
- [55] M. Demuzere, B. Bechtel, and G. Mills, "Global transferability of local climate zone models," *Urban Climate*, vol. 27, pp. 46–63, Mar. 2019, doi: [10.1016/j.uclim.2018.11.001](https://doi.org/10.1016/j.uclim.2018.11.001).
- [56] I. D. Stewart, T. R. Oke, and E. S. Krayenhoff, "Evaluation of the 'local climate zone' scheme using temperature observations and model simulations," *Int. J. Climatol.*, vol. 34, no. 4, pp. 1062–1080, Mar. 2014, doi: [10.1002/joc.3746](https://doi.org/10.1002/joc.3746).
- [57] L. Gawuc, "Diurnal variability of surface urban heat island during a heat wave in selected cities in Poland in August 2013 by means of satellite imagery," *Sci. Papers Warsaw Univ. Technol. Environ. Eng. Ser.*, vol. 68, pp. 19–34, 2014.
- [58] M. Kuchcik, K. Błażejczyk, P. Milewski, and J. Szmyd, "Urban climate research in Warsaw: The results of microclimatic network measurements," *Geogr. Polonica*, vol. 87, no. 4, pp. 491–504, 2014.
- [59] K. Błażejczyk, M. Kuchcik, and P. Milewski, "Commentary on maps of various characteristics of air temperature and precipitation in Warsaw," Jul. 2015, unpublished. [Online]. Available: <http://mapa.um.warszawa.pl/mapaApp1/mapa?service=adaptcity>
- [60] H. Sun, Y. Chen, and W. Zhan, "Comparing surface- and canopy-layer urban heat islands over Beijing using MODIS data," *Int. J. Remote Sens.*, vol. 36, no. 21, pp. 5448–5465, Nov. 2015, doi: [10.1080/01431161.2015.1101504](https://doi.org/10.1080/01431161.2015.1101504).
- [61] J. P. Montávez, J. F. González-Rouco, and F. Valero, "A simple model for estimating the maximum intensity of nocturnal urban heat island," *Int. J. Climatol.*, vol. 28, no. 2, pp. 235–242, 2008, doi: [10.1002/joc.1526](https://doi.org/10.1002/joc.1526).
- [62] J. Hjort, J. Suomi, and J. Käyhkö, "Spatial prediction of urban-rural temperatures using statistical methods," *Theor. Appl. Climatol.*, vol. 106, no. 1, pp. 139–152, Nov. 2011, doi: [10.1007/s00704-011-0425-9](https://doi.org/10.1007/s00704-011-0425-9).

- [63] E. N. Florio, S. R. Lele, Y. Chi Chang, R. Sterner, and G. E. Glass, "Integrating AVHRR satellite data and NOAA ground observations to predict surface air temperature: A statistical approach," *Int. J. Remote Sens.*, vol. 25, no. 15, pp. 2979–2994, Aug. 2004, doi: [10.1080/01431160310001624593](https://doi.org/10.1080/01431160310001624593).

Lech Gawuc received the M.S. degree in remote sensing and photogrammetry and the Ph.D. degree in remote sensing of environment from the Warsaw University of Technology, Warsaw, Poland, in 2011 and 2017, respectively.

His research interest includes urban climate problems, including surface energy balance studies and urban surface temperature analyses. He is currently working on the development of bottom-up emission inventory for Poland.

Dr. Gawuc is a member of Bibliography Committee of International Association for Urban Climate.

Maciej Jefimow has received the bachelor's degree in environmental engineering (specialization in environmental protection techniques and obtained the title of Professional Engineer) and the M.S., and Ph.D. degrees in air quality modelling and aerosol radiative feedbacks from the Warsaw University of Technology, Warsaw, Poland, in 2010, 2012, and 2019, respectively.

Since 2012, he has been participating in national and international projects (e.g., AQMEII phase 1). Currently, he is a Specialist with the Institute of Environmental Protection—National Research Institute, Warsaw, Poland, being involved in climate change oriented projects. He is also employed as a research-and-teaching assistant at the Warsaw University of Technology.

Karol Szymankiewicz received the B.S. and Ph.D. degrees in remote sensing of environment from the Warsaw University of Technology, Warsaw, Poland, in 2010 and 2016, respectively.

He is currently a Specialist with The National Centre for Emissions Management, Institute of Environmental Protection—National Research Institute, Warsaw, Poland. His research interests are connected with GIS methods, remote sensing, air pollution, and emission inventory development.

Magdalena Kuchcik received the Ph.D. degree in earth sciences (geography and climatology) from the Faculty of Geography and Regional Studies, University of Warsaw, Warsaw, Poland, in 2000, and the Postdoctoral degree in geography from Polish Academy of Sciences, Warsaw, Poland, in 2018.

She is currently an Associate Professor with the Climate Impacts Laboratory, Institute of Geography and Spatial Organization Polish Academy of Science, Warsaw, Poland. Her research interests include bioclimatology and biometeorology (impact of weather, climate, and air pollution on health), city climate and bioclimate (urban heat island), as well as local climate of health resorts.

Anahita Sattari received the M.S. degree in environmental protection engineering from the Warsaw University of Technology, Warsaw, Poland, in 2018. She is currently working toward the Ph.D. degree in urban meteorology modelling with the Institute of Geophysics, Polish Academy of Sciences, Warsaw, Poland.

She is a Climate Researcher with the Institute of Environmental Protection—National Research Institute, Warsaw, Poland. Her research interests are connected with urban climate, air quality, climate change, and renewable energies.

Joanna Struzewska received the Ph.D. degree in environmental engineering from the Warsaw University of Technology, Warsaw, Poland, in 2002.

Her research interests are built around numerical modeling of atmospheric processes. She is involved in numerous projects related to air quality, satellite observations of atmospheric composition, and urban climate. She contributes to the Copernicus Atmosphere Monitoring Service—Regional Production (CAMS50). Also, she is responsible for climate change projection analysis for Poland based on EuroCordex in the frame of "Knowledgebase on climate change and adaptation strategies."